2. Atmospheric CO_2 During the Late Paleozoic and Mesozoic: Estimates from Indian Soils

Prosenjit Ghosh, S.K. Bhattacharya, and Parthasarathi Ghosh

2.1 Introduction

Carbon dioxide (CO_2) and water vapor are major greenhouse gases in Earth's atmosphere that control the planet's surface temperature (Houghton and Wood 1989). Variations in CO_2 levels can lead to major changes in climate, surface processes, and biota. For example, over the past two centuries the combustion of fossil fuels has raised the atmospheric CO_2 level from about 275 ppmV (Barnola et al. 1987) to the current level of 365 ppmV (Keeling 1994); this has caused already discernible increases in Earth's near-surface temperature (IPCC 1990). Over a longer timescale, analysis of trapped gases in the polar icecores (Barnola et al. 1987) showed that during the past 150,000 years CO_2 levels have oscillated between approximately 200 and 300 ppmV. Knowledge of past carbon dioxide levels and associated paleoenvironmental and paleoecological changes is useful for predicting future consequences of the current increase in atmospheric CO_2.

While it is possible to directly measure the CO_2 content of the late Pleistocene and Holocene atmosphere, direct estimation of CO_2 levels in the atmosphere is not possible for the pre-Pleistocene epoch.. Several indirect methods (proxy) to estimate the paleo-CO_2 concentration in the atmosphere have been proposed: for example, carbon isotopic analysis of pedogenic carbonates, stomatal index count of fossil leaves, and isotopic composition of marine sedimentary carbon and boron from carbonate fossils (Cerling 1991; McElwain and Chaloner 1996; Ekart et al. 1999; Ghosh, Ghosh, and Bhattacharya 2001; Crowley and Berner 2001). The $\delta^{13}C$ of pedogenic carbonates provide the best $_pCO_2$ estimates for the pre-Tertiary (Royer, Berner, and Beerling 2001). The experimental proxies play an important role in putting constraints on the theoretical models of carbon cycle based on mantle evolution (Tajika and Matsui 1992) and biological and tectonic changes in the past (Berner 1994; Berner and Kothavala 2001), which provide estimates of the atmospheric [CO_2] during the Phanerozoic.

How do paleosol carbonates record the past CO_2 level in the atmosphere? These carbonates are precipitated in the root zone of plants when groundwater supersaturated with carbonate ions can release CO_2 by some process. They are common in regions receiving an annual rainfall of less than 800 mm. The addition of CO_2 in the groundwater during plant respiration and subsequent evaporation and transpiration of water from a plant can induce supersaturation and carbonate precipitation. Paleosol carbonates record the isotopic composition of local soil CO_2, which primarily reflects the type of vegetation (fraction of C_3 and C_4 plants) in the ecosystem (Cerling 1984). The soil CO_2 is a mixture of two components: plant respired CO_2 and atmospheric CO_2. It is important to note that $\delta^{13}C$ of atmospheric CO_2 (about-7‰) is very different from that of soil CO_2 (about-25‰). Atmospheric CO_2 penetrates inside the soil by diffusion and mixes with the soil CO_2 leading to its isotopic change. Today, except for ecosystems with very low productivity, such as deserts, the atmospheric contribution to total soil CO_2 is very small because of very low concentration of CO_2 in the modern atmosphere. However, high atmospheric CO_2 can make a significant contribution to total soil CO_2; in times when few or no C_4 plants were present, this contribution could result in significant isotopic shifts in the $\delta^{13}C$ of soil carbonate precipitated in isotopic equilibrium with soil CO_2. Therefore, $\delta^{13}C$ of pedogenic carbonates can act as a proxy indicator for [CO_2] variations in geologic past (Cerling 1991; Ghosh, Bhattacharya, and Jani 1995; Mora, Driese, and Colarusso 1996; Ekart et al. 1999).

To understand the past [CO_2] variations quantitatively, Berner (1994) proposed the GEOCARB II model based on equations governing the CO_2 outgassing and CO_2 consumption through weathering; he then improved it further in GEOCARB III (Berner and Kothavala 2001). Both of these models predict that in the early Phanerozoic (550 Ma) the [CO_2] was 20 times the present atmospheric level (PAL). Subsequently, the $_pCO_2$ declined in the middle and late Paleozoic (450–280 Ma) to reach a minimum value (approximately similar to the PAL) at about 300 million years ago. The period from 300 to 200 million years ago was again characterized by a rapid rise in the [CO_2] when it increased to 5 times the PAL. Next came a gradual decline, down to the PAL, with a small peak in the early Tertiary. Such large changes in [CO_2] during the geologic past must have had significant influences on the climate, biota, and surface processes of Earth (Berner 1991 and 1997; Mora, Driese, and Colarusso 1996).

The motivation for the present study came from the discovery of well-developed and well-preserved paleosols in the Gondwana sediments of central India; these paleosols cover the period of significant CO_2 change mentioned above in well-spaced intervals. The stable isotopic composition of pedogenic carbonates formed in these paleosols was investigated to decipher the CO_2 concentrations and to compare them with those predicted by the Berner-model.

2.2 Description of Paleosols from Central India

The Gondwana sediments and the overlying Deccan trap of the Satpura basin (Fig. 2.1) of central India range in age from the Permo-Carboniferous to the uppermost Cretaceous.

The thickness of the whole sedimentary succession is about 5 km (Fig. 2.2). The sediments comprise alternate layers of coarse clastics (sandstones along with extrabasinal conglomerates) and fine clastics (red mudstone/carbonaceous shale/white mudstone). The basal unit of this succession is a Permo-Carboniferous glaciolacustrine deposit called the Talchir Formation. The formations overlying the Talchir represent several episodes of fluvial, lacustrine, and alluvial deposition (Robinson 1967; Casshyap and Tewari 1988; Casshyap and Qidwai 1971; Casshyap, Tewari, and Khan 1993; Veevers and Tewari 1995; Ghosh 1997). Occurrences of fossil vertebrates (Chatterjee and Roychowdhury 1974; Mukherjee and Sengupta 1998; Bandyopadhyay and Sengupta 1998) and freshwater

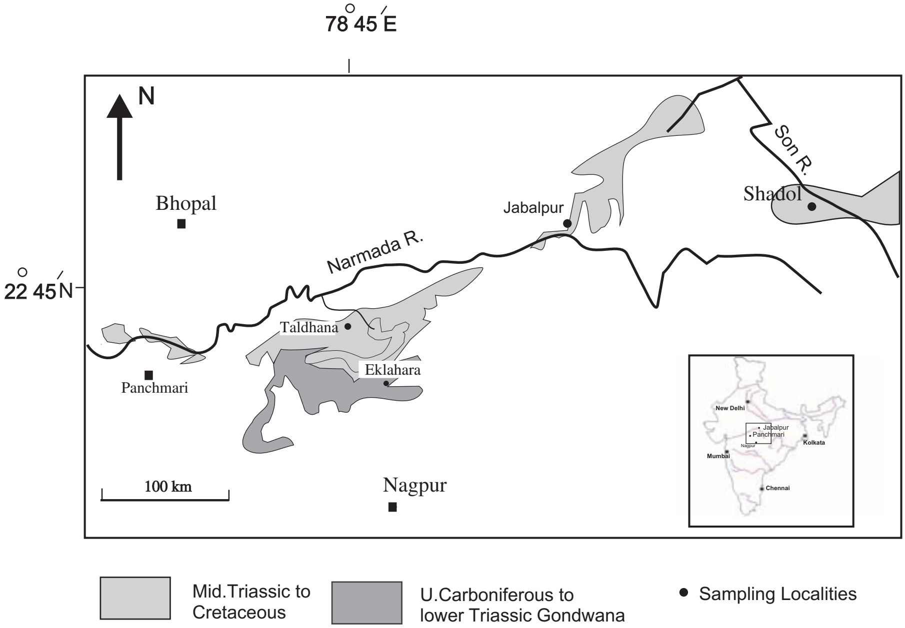

Figure 2.1. Sketch of paleosol locations in the geological map of the Satpura basin and Son Valley basin of the Gondwana supergroup in central India.

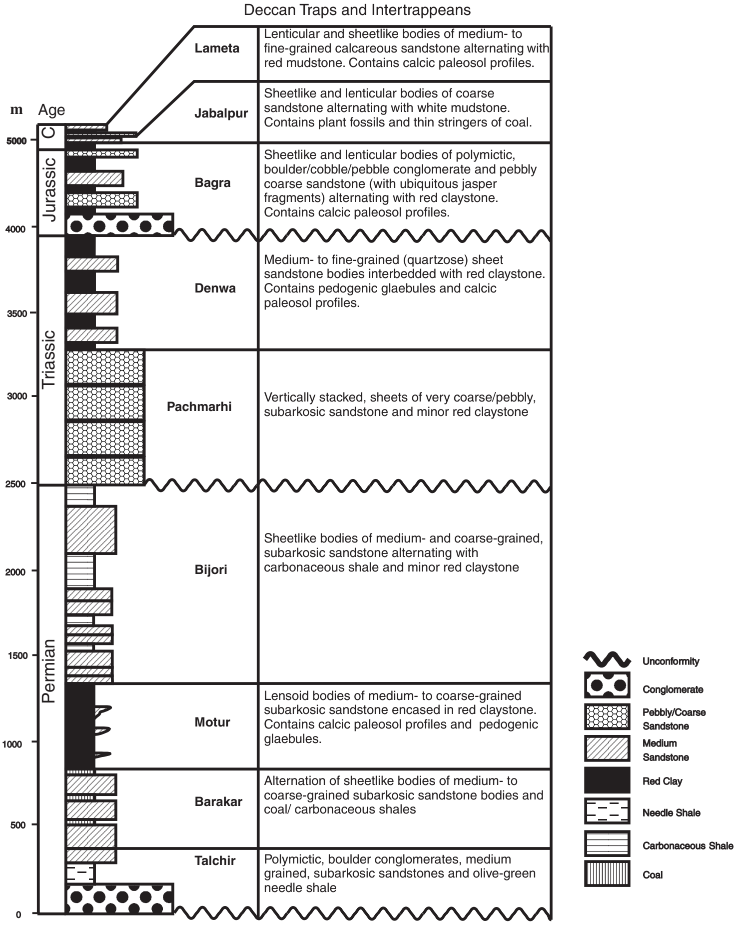

Lameta Lenticular and sheetlike bodies of medium- to fine-grained calcareous sandstone alternating with red mudstone. Contains calcic paleosol profiles.

Jabalpur Sheetlike and lenticular bodies of coarse sandstone alternating with white mudstone. Contains plant fossils and thin stringers of coal.

Bagra Sheetlike and lenticular bodies of polymictic, boulder/cobble/pebble conglomerate and pebbly coarse sandstone (with ubiquitous jasper fragments) alternating with red claystone. Contains calcic paleosol profiles.

Denwa Medium- to fine-grained (quartzose) sheet sandstone bodies interbedded with red claystone. Contains pedogenic glaebules and calcic paleosol profiles.

Pachmarhi Vertically stacked, sheets of very coarse/pebbly, subarkosic sandstone and minor red claystone

Bijori Sheetlike bodies of medium- and coarse-grained, subarkosic sandstone alternating with carbonaceous shale and minor red claystone

Motur Lensoid bodies of medium- to coarse-grained subarkosic sandstone encased in red claystone. Contains calcic paleosol profiles and pedogenic glaebules.

Barakar Alternation of sheetlike bodies of medium- to coarse-grained subarkosic sandstone bodies and coal/ carbonaceous shales

Talchir Polymictic, boulder conglomerates, medium grained, subarkosic sandstones and olive-green needle shale

Figure 2.2. Generalized lithostratigraphy of the Gondwana succession of the Satpura basin. (From Ghosh, Ghosh, and Bhattacharrya 2001, with permission from Elsevier Science.)

bivalves, coupled with such evidences of pedogenesis as the presence of rootlet horizons, paleosol profiles, and so forth (Ghosh, Bhattacharya, and Jani 1995, Ghosh, Rudra, and Maulik 1998; Ghosh 1997; Tandon et al. 1995, 1998) give credence to the alluvial origin of these sediments.

In four litho-formations (the Motur, Denwa, Bagra, and Lameta) of the Satpura basin and one ormation (the Tiki) of the Son Valley basin, preserved calcic paleosols have been identified and characterized (Ghosh, Bhattacharya, and Jani 1995; Ghosh 1997, Ghosh, Rudra, and Maulik 1998; Tandon et al. 1995, 1998; Andrews, Tandon, and Dennis 1995). Stable isotopic compositions of the pedogenic carbonates and associated organic matters from the Motur, Bagra, Denwa, and Lameta formations were investigated in an earlier study (Ghosh,

Ghosh, and Bhattacharya 2001). This chapter describes a more refined analysis of the earlier results and presents an additional analysis of soils from the Tiki Formation. A brief description of the five formations is given below.

2.2.1 Motur Formation

The Motur Formation is a 700 m thick succession of fluvial channel sandstone bodies alternating with floodplain complexes made up of red claystone and thin sandy splay deposits. In the middle part of the Motur succession a few calcic paleosols occur within the floodplain deposits. These paleosols are characterised by three to four vertically superposed distinct pedo-horizons forming paleosol profiles (Fig. 2.3A).

Two types of profiles can be recognized. One type is around 50 cm thick, whereas the other is thicker (3–4 m). The thinner variety comprises an uppermost horizon (3–5 cm thick) of coalesced platy globules overlying a 10 to 30 cm thick horizon of closely spaced vertically oriented rhizocretions (Fig. 2.3B).

The rhizocretion horizon grades downward to a horizon with profuse subspherical globules that overlies a gleyed horizon. The uppermost horizon of fused platy globules is similar to the K horizon of modern aridisols whereas the zones of rhizocretions and globules can be compared with the Bk soil horizons (Soil Survey Staff 1975).

The thicker paleosol profiles show a meter-thick upper zone with a number of curved, mutually intersecting inclined surfaces (see Fig. 2.3A), coated with centimeter-thick carbonate layers, within a red claystone host. The underlying horizon is characterized by small, subvertical, dispersed, calcareous rhizocretions. Underneath this horizon is a thin (3–5 cm thick) horizon of subspherical globules overlying a gleyed horizon (~20 cm thick).

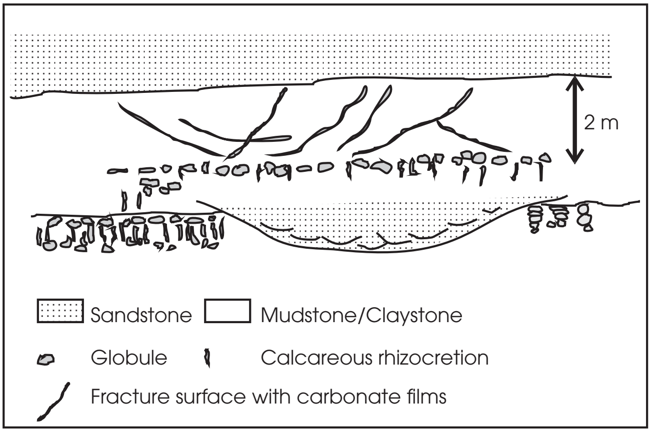

Figure 2.3A. Field sketch of the two vertically superposed calcic paleosol profiles of the Motur Formation, exposed near Eklahara colliery.

Figure 2.3B. Close-up of globular horizon (Motur Formation, near Eklahara colliery).

The curved inclined surfaces, within the clayey host, in the upper part of these paleosols resemble the zone of pedogenic slickensides (ss horizon) that develop in modern vertisols in response to shrinking and swelling of the soil clay matrix. The underlying horizons of rhizocretions and globules can be compared with modern Bk horizons. The field features of these paleosol profiles are similar to the Appalachian Paleozoic vertic paleosol profiles described by Driese and Mora (1993) and Mora et al. (1998).

A total of 21 samples were collected from the Motur Formation near Eklahara colliery (22°12'N, 78°41'E). Studies on the vertic paleosols have demonstrated that the globules occurring within the vertic horizons are enriched in ^{13}C compared to those occurring below the vertic horizons and compared to the rhizocretions in general (Driese and Mora 1993; Mora, Fastovsky, and Driese 1993). The cracks that develop in the vertic soils in response to the shrinking and swelling of the soil clay matrix possibly allow direct and nondiffusive penetration of the heavier atmospheric CO_2 deeper down the soil; hence, samples from this horizon may provide an incorrectly high estimate of the atmospheric CO_2. The vertic paleosols, therefore, were sampled for rhizocretions and globules from the horizons that occur considerably below the horizon of slickensides and above the gleyed zone. For the thinner paleosols, samples of rhizocretions and globules were collected from the basal part of the horizon of rhizocretions and the underlying horizon of globules. The horizons of platy globules were not sampled; thus, the studies avoided a possible anomalous large contribution of atmospheric CO_2 near the soil-to-atmosphere contact (Cerling 1984, 1991).

2.2.2 Denwa Formation

The Denwa Formation is about 600 m thick at its maximum. The lower half of the formation is characterized by a regular alternation of medium- to fine-grained, thick (3–15 m) fluvial channel sandstone bodies and floodplain deposits. The floodplain deposits comprise red mudstones intercalated with centimeter-to-decimeter thick, fine-grained sandstone layers. In contrast to the lower part of the formation, the upper half is fines-dominated. The red mudstones encase

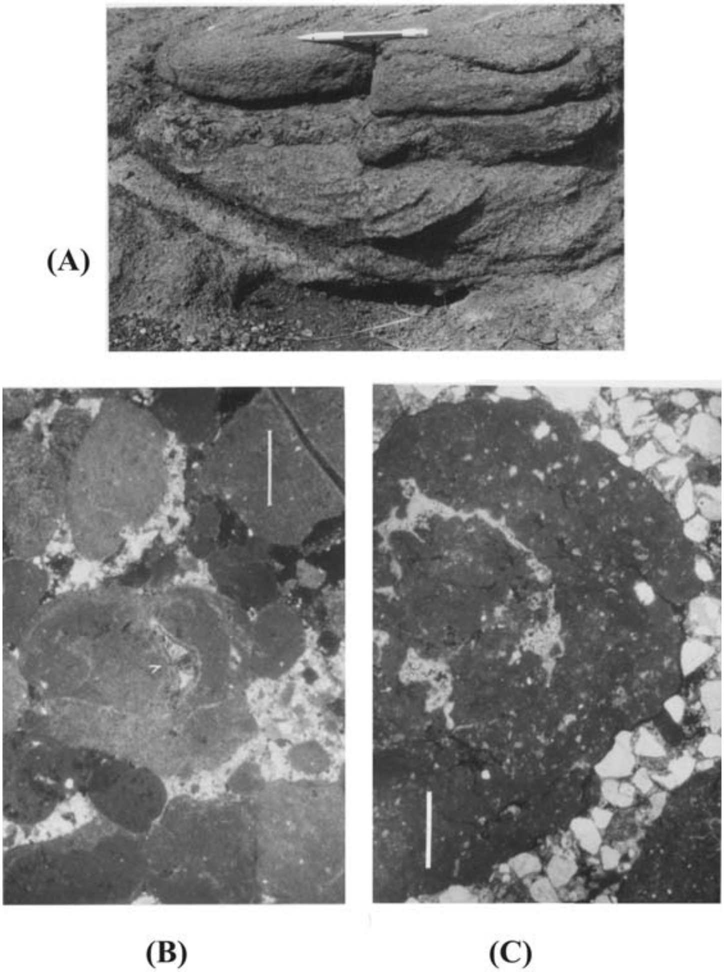

Figure 2.4. **(A)** Close-up of a trough cross-stratified channel-fill deposit, made up of pedogenic globules within the upper part of the Denwa Formation. **(B)** Photo-micrograph of pedogenic globules; note the spar-filled cracks within the calcareous matrix of the globules. Scale bar = 0.8 mm. **(C)** Photomicrograph of a globule; note the sharp and rounded outline of the globule and the spar-filled (lighter) circum-granular crack. Scale bar = 1 mm. (**C** from Ghosh, Ghosh, and Bhattacharrya 2001, with permission from Elsevier Science.)

fine-grained (fine sandstones and siltstones) point bar deposits that are 2 to 4 m thick and lenticular channel-fill bodies that are about 1 m thick. Detrital subspherical globules that are the size of pebbles to coarse sand constitute the bulk of these channel-fill bodies. These bodies are internally trough cross-stratified (Fig. 2.4A).

Microscopic observations of the detrital globules reveal that they are composed mostly of micrite and minor microspar with one or two sand-sized detrital quartz grains floating in the carbonate groundmass (Fig. 2.4B).

A number of globules show radial fractures filled with either blocky spars or barite. Spar-filled, circum-granular cracks also have been noted in some of the globules along with such pedogenic features as clotted micrite and corroded detrital quartz grains (Fig. 2.4B,C).

The field occurrence of paleosols in the Denwa Formation is limited, and only the widespread occurrence of detrital globules with pedogenic microfabrics provides indirect evidence of pedogenesis during the later part of the Denwa sedimentation. However, exposed paleosols with two distinct pedohorizons can be studied in a single exposure. The profile is more than 4 m thick. Its upper 2 to 3 m is characterized by a number of inclined and mutually intersecting nearly planer surfaces and dispersed globules the size of small pebbles to coarse sand and pale yellow blotches. Larger inclined features are about 5 m long and 5 to 7 cm thick, whereas the length of the smaller ones is 1 to 2 m and these are less than a centimeter thick. Large inclined features are filled with calcareous very fine sandstone. The surfaces of the smaller inclined surfaces have a polished appearance and are, at places, coated by 1 to 5 cm thick carbonate layers. This horizon passes gradually to an underlying horizon of numerous isolated pebble-sized globules, small (2–7 cm long) calcareous rhizocretions and pale yellow-gray mottles. The larger inclined features of the overlying horizon, however, cut across the lower horizon. The discordant relationship between the horizons and the large inclined features along with their sandy fills suggest that these are possibly desiccation cracks. The smaller inclined features can possibly be equated with the pedogenic slickensides noted in the upper part of the modern day vertisols (Soil Survey Staff 1975). The lower horizon represents the zone of carbonate accumulation at a deeper part of the soil. The macroscopic characters of the Denwa paleosol profiles are also similar to the Appalachian vertic paleosols (Driese and Mora 1993; Mora et al. 1998).

Nineteen samples of soil carbonates were collected from the formation (see Fig. 2.4D). The bulk of the samples comprise detrital pedogenic globules of the channel-fill bodies (between 22°38'N, 78°20'E and 22°35'N, 78°38'E). The rhizocretions and globules from the basal horizon of the paleosol near Taldhana village (22°37'N, 78°32'30"E) also were sampled.

2.2.3 Tiki Formation

The Tiki Formation is a 1200 m thick succession of fluvial channel sandstone bodies alternating with floodplain complexes made up of shale and thin sandy floodplain deposits. Floodplain deposits consist essentially of bright red colored

Figure 2.4D. A vertic paleosol profile of the Denwa Formation, exposed near Taldhana village showing a zone of well-developed vertical rhizocretions (R) overlying a zone of subspherical calcareous globules (G). Each division of scale bar is 50 cm.

clays, interbedded with soft, light colored sandstone. There are three different types of paleosols occurring in the area. Type I shows calcareous rhizocretions in a host of medium- to fine-grained, cross-stratified fluvial channel sandstone deposit (Fig. 2.5A).

Most of the concretions are rhizocretions with a few subspherical globules. The majority of the rhizocretions are subvertical, whereas the rhizocretions occurring near the top are typically subhorizontally aligned. Type II shows the development of calcareous globules and a few rhizocretions in the red mudstone/siltstone of the floodplain deposits associated with the fluvial channels (Fig. 2.5B).

The majority of the concretions are subspherical and platy globules, and, in contrast to type I, rhizocretions are rare. Type III paleosol (Fig. 2.5C) shows cross-bedded detrital calcareous concretions at the basal part of a sandy fluvial channel deposit. These are immature aridisols or calcisols with only a partially modified host at the base (C horizon) and a weakly developed Bk on top of it.

Nine samples of soil carbonates were collected from the fFormation. The bulk of the samples comprise detrital pedogenic globules of the channel-fill bodies, the rhizocretions, and globules from the basal horizon of the paleosol near Beohari village, 12 km north of Shadol district, Madhya Pradesh (21°N, 81°30 E; see Fig. 2.1).

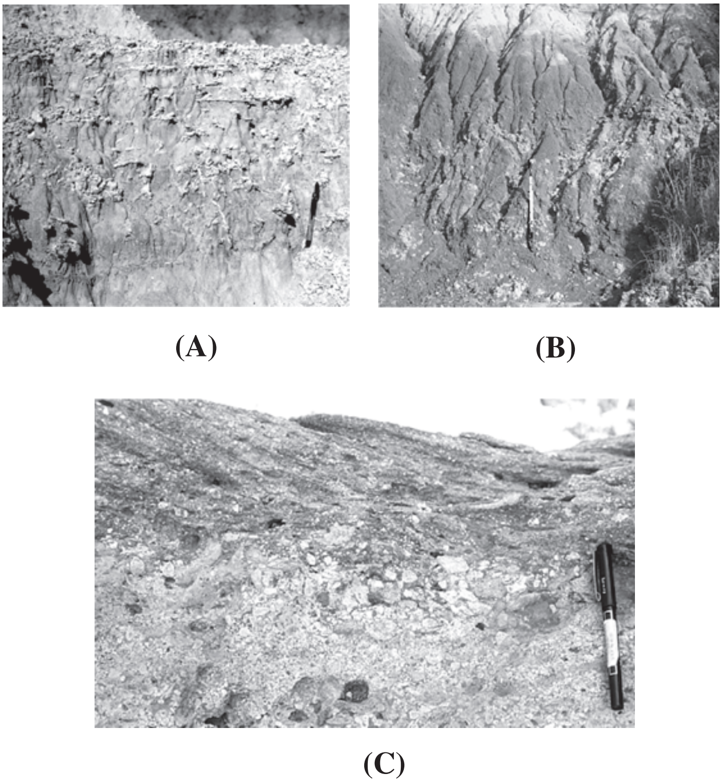

Figure 2.5. **(A)** Calcareous rhizocretions in a host of medium- to fine-grained, cross-stratified fluvial channel sandstone deposit. Most of the concretions are rhizocretions with a few subspherical globules. Majority of the rhizocretions are subvertical, whereas the rhizocretions occurring near the top are typically subhorizontally aligned. **(B)** Development of calcareous globules and a few rhizocretions in the red mudstone/siltstone of the floodplain deposits associated with the fluvial channels. Majority of the concretions are subspherical and platy globules (scale is 1.5 m in length). **(C)** Cross-bedded detrital calcareous concretions at the basal part of a sandy fluvial channel deposit.

2.2.4 Bagra Formation

The Bagra Formation is 250 to 500 m thick. Thick units of polymictic conglomerates and pebbly sandstones, interbedded with red claystone units, characterize this formation. The internal architecture of the clastic bodies indicates that most of them were deposited within the channels of braided streams, whereas the claystones were formed in the associated floodplains. The paleosol profiles are associated mainly with these floodplain deposits and are found in the lower half of the formation. At places, pedogenic modification extended up to the coarse-grained abandoned channels and the wings of the main channel

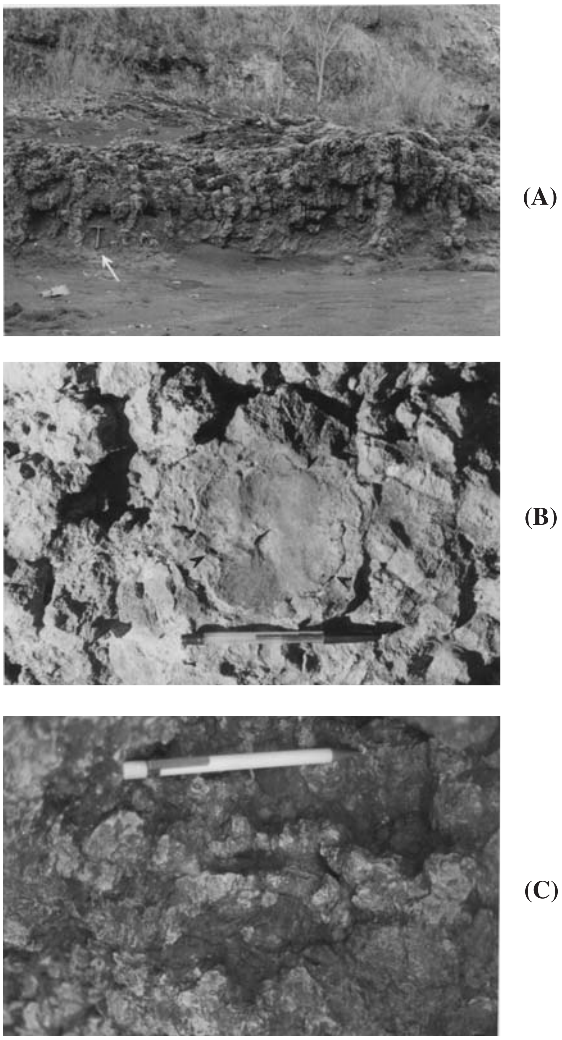

Figure 2.6 **(A)** Calcic paleosol profile of the Bagra Formation; note a horizon of coalesced globules in the upper part of the profile and a zone of well-developed, vertical rhizocretions in the lower part (hammer included for scale). **(B)** Bedding plane view of a rhizocretion associated with paleosol profile of the Bagra Formation. The outline of the rhizocretion is marked by arrows; note the coaxial zonation within the rhizocretion. **(C)** Transverse section through a rhizocretion; note the slightly tortuous shape of the central zone of the rhizocretion (pen included for scale). (**A**, **B**, and **C** from Ghosh, Ghosh, and Bhattacharrya 2001, with permission from Elsevier Science.)

bodies. The paleosol profiles are 70 cm to 2 m thick. They are characterized by a 10 to 50 cm thick well-developed horizon of fused calcareous globules at the top (Fig. 2.6A).

A thick to very thick (50 cm to 1.5 m) horizon of closely spaced, vertically oriented, large cylindrical rhizocretions occurs below the top globule horizon. The cross-sectional diameter of the rhizocretions ranges from 3 to 5 cm; the length ranges from 30 to 100 cm. The rhizocretions internally show two distinct coaxial cylindrical regions with a sharp contact in between (Fig. 2.6B,C).

The inner region (1–2.5 cm in cross-sectional diameter) comprises large spars and minor carbonaceous clays (Fig. 2.6C). The outer region is made up of reddish gray micritic limestone. The field features of the paleosol profiles of the Bagra Formation are comparable to the present-day aridisols with a well-developed K-horizon at the top and a thick Bk horizon below it (Soil Survey Staff 1975).

A total of 29 samples from the rhizocretions and pedogenic globules were collected from different paleosol profiles of the Bagra Formation between 22°35'N, 78°18'E and 22°40'N, 78°37'30"E (see Fig. 2.1).

2.2.5 Lameta Formation

Lameta beds represent an extensive lacustrine-palustrine deposit occurring as discontinuous patches along the Narmada lineament in central India below the Deccan basalts. Diverse freshwater and terrestrial fossils are reported from the Lameta beds; the most important are dinosaur skeletal remains and eggshells (Sahni et al. 1994; Sarkar, Bhattacharya, and Mohabey 1991). The present section is located at Lameta Ghat on the Narmada River, 15 km southwest of Jabalpur. Here, fluviatile sediments that are about 35 m thick transitionally overlie fluvial sandstone and mudstone facies of Cretaceous Jabalpur Formation. A number of calcic paleosols, stacked vertically, have been recorded in the Lameta Formation. Ghosh (1997) suggested that development of the calcic paleosols took place in alternation with fluvial depositional events. The paleosol profile shows vertical root traces, and globules occur where the water table was low. More details of Lameta Formation are given in Ghosh, Bhattacharya, and Jani (1995) and Tandon and Andrews (2001).

2.3 Reappraisal of Paleosol Ages

The importance of uncertainty regarding the ages of these strata became apparent when we compared our pCO_2 estimates of paleosols from the four stratigraphic horizons of the Satpura Valley basin (Ghosh, Ghosh, and Bhattacharya 2001) with the revised model curve (GEOCARB III) of Berner and Kothavala (2001). Ghosh, Ghosh, and Bhattacharya (2001) found a major discrepancy between predicted values and pCO_2 estimates in the case of Jurassic (Bagra) and Cretaceous (Lameta) paleosols, which prompted us to do a reappraisal of the ages.

The age estimates of the Satpura soils are based mainly on the paleontological records and allow a great deal of uncertainty. It is crucial to ascertain the nature and extent of uncertainty of the soil ages to compare our observations with the predictions. We discuss below our earlier consideration and present understanding based on available literature.

The ages of the soils studied here are derived from faunal remains of vertebrates and microfossils, such as diatoms. Additional clues are obtained by considering the stratigraphic position of soil horizons with respect to strata of known ages. A literature survey indicates the following ages (with uncertainty) for Motur, Denwa, and Lameta formations: early middle Permian (275 ± 15 million years ago), middle Triassic (235 ± 5 million years ago), and late Cretaceous (80 ± 15 million years ago), respectively (Raja Rao 1983; Bandyopadhyay and Sengupta 1998; Casshyap, Tewari, and Khan 1993; Satsangi 1988; Chatterjee and Roychowdhury 1974). In the case of the Bagra Formation, the absence of fossil records was confounding. Several workers contended that it might be considered either equivalent to or younger than Denwa (Sastry et al. 1977). Since the age of the Denwa beds is thought to be between late Lower Triassic and middle Triassic (Chatterjee and Roychowdhury 1974), the age of Bagra was thought to be around late Triassic (Singh and Ghosh 1977). However, Casshyap, Tewari, and Khan (1993) studied the field relationship of Bagra Formation with the underlying Denwa sequence in central India and based on various lines of stratigraphic, tectonic, and sedimentologic evidence suggested that the Bagra Formation should be younger than late Triassic but older than or equivalent to late Jurassic to early Cretaceous. We now consider the Bagra Age as 175 ± 30 million years ago instead of the 200 million years ago (Jurassic) adopted earlier (Ghosh, Ghosh, and Bhattacharya 2001). The Tiki shale bed yielded a rich microfloral assemblage equivalent to upper Triassic microfloral elements (Sundaram, Maiti, and Singh 1979). In addition, it contains reptile fossils of Carnian Age (Anderson 1981; Kutty, Jain, and Roychowdhury 1998; Sengupta 1992). The upper part of the sedimentary sequence is dated as Carnian-Norian (210 million years ago) on the basis of vertebrate fossil evidence. Therefore the age of Tiki Formation is considered to be middle to upper Triassic, 225 ± 15 million years ago (Dutta and Das 1996).

2.4 Analytical Procedures

The thin sections of the samples were carefully studied to identify portions rich in pedogenic micrite so that sparite-rich portions could be avoided. Micritic-rich parts of the samples were thoroughly cleaned with deionized water in an ultrasonic bath. XRD analysis of fine-grained powders showed dominance of calcite with subordinate clays and detrital quartz grains. A few milligrams of powdered samples were reacted with 100% orthophosphoric acid at 50°C in a vacuum using an online extraction system (Sarkar, Ramesh, and Bhattacharya 1990). The evolved CO_2 gas was thoroughly purified and analyzed in a VG 903 mass spectrometer. Some of the samples were analyzed in a GEO 20-20 dual inlet mass spectrometer at 80°C using an online CAPS extraction system. Calibration and checkup of the system were done using NBS-19.

In order to determine the $\delta^{13}C$ value of organic matter associated with the soil carbonates, powdered samples were treated with 20% HCl for 24 hours to remove the carbonates. Dried residue was loaded in a 10cm long quartz break seal tube along with CuO (wire form) and Ag strip. The quartz tube was evacuated, sealed, and combusted at 700°C for 6 hours. Evolved CO_2 was purified and analyzed using GEO 20-20 IRMS. To check the reproducibility of measurements, UCLA glucose standard was analyzed along with each set of samples. Many of the samples were re-analyzed to check the homogeneity of the samples. Isotopic ratios of carbon and oxygen are presented in the usual d notation in units of per mil (‰) with respect to international standard V-PDB and V-SMOW, respectively, and are reproducible within $\pm 0.1‰$ at 1σ level.

2.5 Observations

The detailed results of isotopic analysis of soil carbonates from Motur, Denwa, and Bagra formations are given in Ghosh, Ghosh, and Bhattacharya (2001), and the mean $\delta^{18}O$ values (excluding a few outliers that deviate by more than 2σ) are 18.2‰ (σ = 0.9‰), 24.2‰ (σ = 0.7‰), and 24.1‰ (σ = 0.8‰), respectively. The corresponding mean $\delta^{13}C$ values are as follows: −6.5‰ (σ = 0.8‰), −6.7‰ (σ = 0.5‰), and −6.1‰ (σ = 0.8‰), respectively. The $\delta^{18}O$ and $\delta^{13}C$ values of all the samples are distributed (Fig. 2.7) such that except for a few outliers the values are closely clustered around their respective means.

The mean values for pedogenic carbonate samples from the Lameta Formation (Ghosh, Bhattacharya, and Jani 1995) are: 24.7‰ for $\delta^{18}O$ and −9.1‰ for $\delta^{13}C$. The mean $\delta^{13}C$ values of organic matter associated with the paleosols are: −23.5‰ (σ = 0.5‰) for the Motur Formation, −24.6‰ (σ = 0.5‰) for the Denwa Formation and −26.1‰ (σ = 1.2‰) for the Bagra Formation. Organic matter from a single sample of the Lameta soil yielded a value of −27.3‰. Andrews, Tandon, and Dennis (1995) reported $\delta^{13}C$ values of −22.1‰ and −17.1‰ for two samples of organic matter from the Lameta Formation. These latter values are somewhat inconsistent with the normal range of C_3 plants and, therefore, not considered here. The results of isotopic analysis of soil carbonates from the Tiki Formation are given in Table 2.1. The mean $\delta^{18}O$ value for the Tiki samples (excluding the outliers that deviate by more than 2σ) is 26.1‰ (σ = 1.2‰). The corresponding mean $\delta^{13}C$ value is −6.9‰ (σ = 0.8‰) for carbonates and −24.7‰ (σ = 1.2‰) for associated organic matter.

In order to derive paleoclimatic information from the stable isotopic composition of paleosol carbonate and organic matter, it is necessary to establish that the samples have not undergone any postdepositional alteration. The fine-grained fabric in the samples and the dominance of pedogenic micrite along with general absence of sparry calcite rule out major recrystallization subsequent

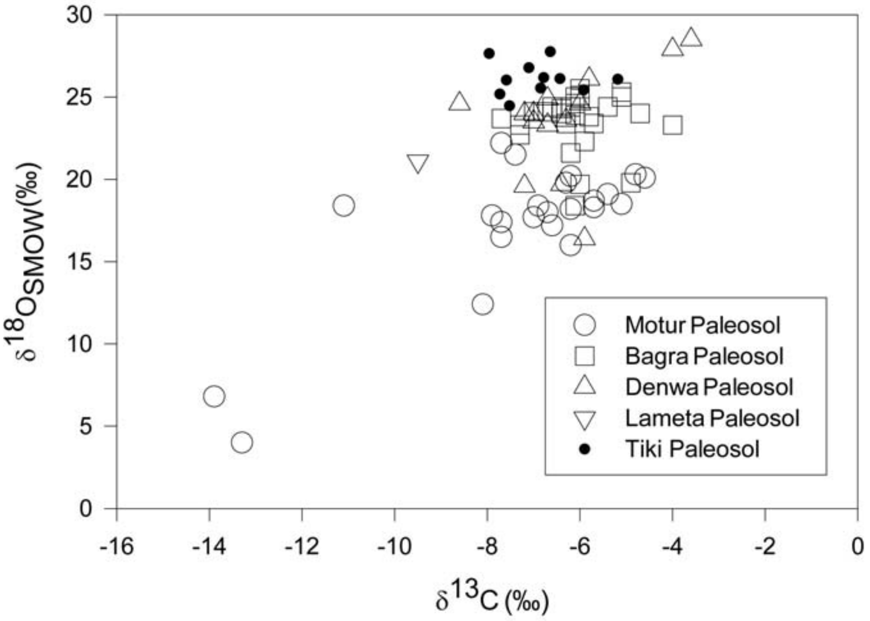

Figure 2.7. Plot of $\delta^{18}O$ versus $\delta^{13}C$ values of the pedogenic carbonates from the Motur, Denwa, Tiki, Bagra, and Lameta formations.

Table 2.1. Carbon and oxygen isotopic composition of pedogenic carbonate and $\delta^{13}C$ of soil organic matter from the Tiki Formation (middle Triassic)

Sample	$\delta^{13}C$, ‰	$\delta^{18}C$, ‰	$\delta^{13}C_{org}$, ‰
TK-21	−6.6	−3.1	−24.2
TK-37	−7.1	−4.1	−25.0
TK-2	−6.4	−4.7	
TK-22	−7.5	−6.3	−22.1
TK-15/4	−7.6	−4.8	
TK-16	−6.8	−5.3	−25.2
TK-28	−7.7	−5.6	
TK-20	−5.9	−5.4	−25.3
TK-18	−5.2	−4.7	
TK-3	−6.8	−4.7	−25.6
TK-14	−8.0	−3.2	−25.2
Mean ± standard deviation	−6.9 ± 0.8	−4.7 ± 1.0	−24.7 ± 1.2

to the precipitation of original carbonate. The isotopic data also show only minor spread in carbon and oxygen isotopic composition (see Fig. 2.7) among various samples from the same formation (except in a few outliers which are probably due to diagenetic alteration). The consistency in isotopic composition within 1‰ would be unlikely if alteration affected majority of the samples. Additionally, our results are comparable with the published data of other workers on soil carbonates of similar ages and environments (Cerling 1991; Yapp and Poths 1992; Mora, Driese, and Colarusso 1996).

The observed $\delta^{13}C$ values of the organic matter associated with the pedogenic carbonates lie within a range that closely matches that of the C_3 vegetative biomass. Because all the samples are from horizons older than Miocene (when C_4 plants were absent), these values provide additional evidence against any late diagenetic modifications. Moreover, the differences in $\delta^{13}C$ between coexisting organic matter and carbonate have a range (14‰–20‰) similar to that obtained for other paleosol samples of similar age (Mora, Driese, and Colarusso 1996).

2.6 Model for Estimation of Atmospheric pCO_2

Cerling's (1991) paleobarometer model is basically an isotopic mixing model where the soil-CO_2 is made up of atmospheric CO_2 (through diffusion) and plant-respired CO_2 from vegetative sources. Since this plant-respired CO_2 flux dominates, soil CO_2 in well-aerated soils can be modeled as a standard diffusion-production equation (Baver, Gardner, and Gardner 1972; Kirkham and Power 1972; Cerling 1984):

$$\frac{\partial C_s}{\partial t} = D_s \frac{\partial^2 C_s}{\partial z^2} + \phi_s (z) \tag{2.1}$$

where C_s = soil CO_2 (molecule cm^{-3}), t = time, z = depth in the soil profile (cm), and $\phi_s(z)$ = CO_2 production rate as a function of depth (molecule sec^{-1} cm^{-3}), D_s is the diffusion coefficient, and ϕ_s is the production function with respect to the depth z (Cerling 1984). Solving this equation with a no-flux boundary at depth and Cs (at z =0) set equal to atmospheric carbon dioxide yields:

$$C_s (z) = S(z) + C_a \tag{2.2}$$

where $S(z)$ is CO_2 contributed by soil respiration, and C_a is atmospheric CO_2. Cerling (1984, 1991) solved this equation for ^{12}C and ^{13}C and showed that the isotopic composition of soil CO_2 is controlled by diffusion process (diffusion of CO_2 from soil to atmosphere) and CO_2 production. In a paleosol, $CaCO_3$ precipitates in equilibrium with soil CO_2, which is modified by atmospheric contribution, thus allowing the $\delta^{13}C$ value of carbonate to be used for atmospheric [CO_2] calculation. The solution to the soil CO_2 equation of Cerling (1984, 1991, 1999) can be recast in terms of the isotopic composition of atmospheric CO_2:

$$C_a = S(z)\,\frac{\delta^{13}C_s - 1.0044\delta^{13}C_\phi - 4.4}{\delta^{13}C_a - \delta^{13}C_s} \tag{2.3}$$

under the assumption that ${}^{12}C_s/{}^{13}\,C_a \approx C_s/C_a$ where $\delta^{13}C_s$, $\delta^{13}C_\phi$ and $\delta^{13}C_a$ are the isotopic compositions of soil CO_2, soil respired CO_2 and atmospheric CO_2 respectively. The term *S(z)* is a function of depth but approaches a constant value below about 20 to 30 cm in depth (Cerling 1984; Cerling and Quade 1993). Soil CO_2 is enriched in ${}^{13}C$ relative to respired CO_2 by 4.4‰ due to mass dependent rate of diffusion (Cerling 1984), independent of CO_2 concentration.

The $\delta^{13}C$ of soil carbonate is governed by the $\delta^{13}C$ value of the soil CO_2 and fractionation during precipitation, which is temperature dependent (Deines, Langmuir, and Harmon 1974). The $\delta^{13}C$ values of the two sources of soilCO_2 (e.g., respiration and atmosphere) are quite different. Whereas the recent pre-industrial atmospheric CO_2 is −6.5‰, the CO_2 respired by C_3 type vegetation can have value between −20‰ and −35‰, with a mean around −27‰ (Ehleringer 1989). The degree of infiltration of the atmospheric CO_2 in the soil matrix (which is dependent on the atmospheric $[CO_2]$) thus influences the $\delta^{13}C$ value of the soilCO_2 and consequently the $\delta^{13}C$ value of the pedogenic carbonate. Therefore, this model allows us to estimate the $[CO_2]$ values of the ancient atmosphere from the $\delta^{13}C$ value of the pedogenic carbonates if the following parameters are known:

1. The temperature of calcite precipitation in the soil
2. The $\delta^{13}C$ value of the plant-respired CO_2
3. The $\delta^{13}C$ value of the atmospheric CO_2
4. The difference between the concentration of the soil pCO_2 and the atmospheric pCO_2

We discuss below the procedures for estimating each of these parameters.

2.6.1 Estimation of Soil Temperature

Estimation Based on Paleolatitude. The temperature of the calcite precipitation in the soil is close to the mean soil surface temperature. Scotese (1998) surmised that the Permian was a period during which large global temperature changes took place. In the early Permian, global temperature was low with a mean around 10°C; at the end of the Permian, the temperature was extremely high, near about 35°C (Scotese 1998). The global temperature was maintained at a slightly reduced value of 30°C till the middle Jurassic. The widespread glacial deposits at the Permo-Carboniferous boundary (Talchir Formation) followed by thick coal deposits of the overlying Barakar Formation (see Fig. 2.2); the occurrence of red beds and calcic paleosols in the Motur, Denwa, Tiki, and Bagra Formations; and the presence of thick deposits of carbonaceous claystones in the Bijori Formation (late Permian), all comprise constitute supporting evidence for the suggested trend of the global temperature. However, the surface temperature of a locality is also influenced by its altitude and latitudinal position. The paleo-

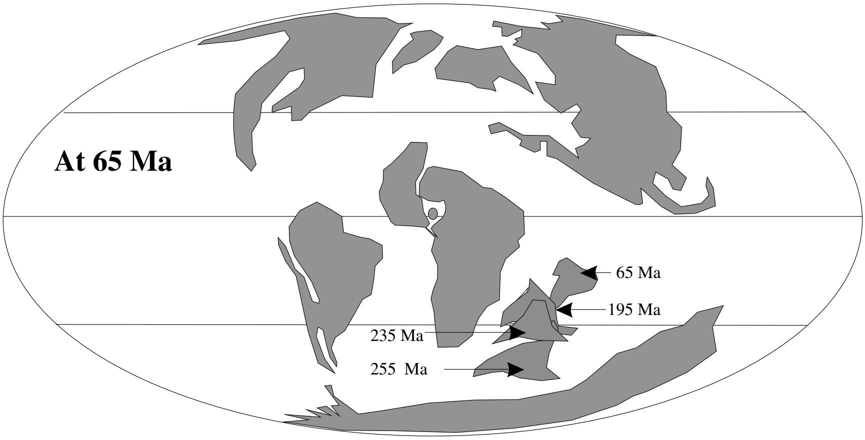

Figure 2.8. Reconstruction of palaeolatitude of India between 255 and 65 Ma as proposed by Scotese (1997). The figure also shows the distributions of the ocean basins and continents at 65 Ma.

geographic reconstructions of the Gondwana landmasses indicate that the study area was situated at 60°S during the Permian (275 ± 15 million years ago), at 50 to 40°S during the middle to upper Triassic (240–205 million years ago), and at 25°S during the late Jurassic to early Cretaceous (175 ± 30 million years ago), as shown in Fig. 2.8. During this period the altitude seems to have remained consistently low and probably close to the sea level (Scotese 1997).

The temperature of soil carbonate precipitation in the present case can be inferred based on the latitudinal position of the Indian landmass during Paleozoic and Mesozoic periods and by using the global data set relating latitude and average temperature (IAEA/WMO 1998). We assume that the major part of the soil carbonate precipitates at the maximum possible temperature at a given latitude. The paleosols described in this study were formed in paleolatitude range of 60°S to 25°S. Modern growing season temperature close to sea level in these latitudes typically ranges from 10° to 30°C. A scatter plot of maximum monthly temperature for the 60°S to 25°S latitudes reveals that 20°C is a typical temperature at 60°S while for 45°S to 25°S one can consider 25°C as representative (see Fig. 5 of Ekart et al. 1999). We have, therefore, chosen 20°C as the temperature of soil carbonate precipitation for the Motur Formation and 25°C for the Denwa, Tiki, and Bagra formations.

Estimation Based on Oxygen Isotope Ratios. An independent estimate of surface temperature can be obtained based on $\delta^{18}O$ values of the carbonates and composition of the ancient soil water in these locations. Soil water is derived from precipitation the composition of which depends on the latitude and the composition of the ocean water. The average $\delta^{18}O$ values of the present-day rainfall at 60°S, 45°S, and 25°S are available from the compilation of Rozanski, Araguas, and Gonfiantini (1993). The $\delta^{18}O$ of the ocean water during the Permian, Triassic, and Jurassic periods was slightly less and commonly assumed to be −1‰ (Veizer, Fritz, and Jones 1986). Assuming that the global moisture circulation was similar to that of today, one can estimate the composition of the precipitation at those locations and times (Table 2.2).

However, a correction is needed for the Permian Period (Motur soil) because, according to Kutzbach and Gallimore (1989), a megamonsoonal circulation operating at that time gave intense seasonal precipitation. We estimate a 2.5‰ depletion in the $\delta^{18}O$ value due to attendant amount effect in the rainfall based on difference in rainfall during the Permian (Kutzbach and Gallimore 1989) and today (Rozanski, Araguas, and Gonfiantini 1993). Similarly, a depletion of 3‰ was postulated for the Lameta Period due to continental effect (Ghosh, Bhattacharya, and Jani 1995). Using these values and an enrichment of 2‰ due to evapotranspiration (Ghosh, Bhattacharya, and Jani 1995) during conversion of rainwater to soil water, one can estimate the soil temperatures during these four periods (see Table 2.2). The values are 17°, 17°, 23°, and 25°C, respectively, and are in reasonable agreement with the estimates derived in the preceding paragraph.

The above method of estimating the soil temperature is critically based on the assumption that no significant diagenetic alteration took place that could have changed the original $\delta^{18}O$ of the carbonate. For example, an increase of approx 1‰ in $\delta^{18}O$ due to postdepositional diagenesis would imply a approx 4°C decrease in temperature estimate leading to reduction in the [CO_2] estimate by about 20% (Cerling 1999; Ekart et al. 1999).

Table 2.2. Estimation of CO_2 concentration and its isotopic composition in the atmosphere at different times in the past

Formation Age (My)	$\delta^{13}C$ (carbonate)	$\delta^{13}C$ (OM)	Temperature (°C)	$\delta^{13}C$ of atmospheric CO_2, ‰@	pCO_2† A	B	Atmospheric CO_2 (ppmV)
MOTUR (275 ± 15)	−6.5	−23.5	20	−2.5	540	890	715
DENWA (235 ± 5)	−6.7	−24.6	25	−3.6	910	1510	1210
TIKI (225 ± 15)	−6.9	−24.7	25	−3.7	880	1460	1170
BAGRA (175 ± 30)	−6.1	−26.1	25	−5.1	1675	2775	2225
LAMETA (80 ± 15)	−9.1	−27.6	25	−6.6	1110	1850	1480

@ $\delta^{13}C$ of atmospheric CO_2 obtained by subtracting 21‰ from $\delta^{13}C$ (OM) (see text).

† Column A and B refer to $S_{(z)}$ values of 3000 and 5000 ppm in Cerling's model, respectively (see text).

2.6.2 $\delta^{13}C$ of the Plant-Respired CO_2

The $\delta^{13}C$ value of the organic matter associated with each soil was determined in this study to act as a suitable proxy for the $\delta^{13}C$ of plant-respired CO_2 in that soil environment. Prior to the Miocene, C_4 plants were not present in the ecosystem; C_3 plants were the dominant vegetative biomass. The $\delta^{13}C$ values of the plant-respired CO_2 of the modern C_3 plants range from −20‰ to −35‰ with an average of −27‰ (Ehleringer 1989). The mean $\delta^{13}C$ values of −23.5‰, −24.6‰, −24.7‰, −26.1‰, and −27.6‰ for the Motur, Denwa, Tiki, Bagra, and Lameta Formations (see Table 1.1) lie close to the mean $\delta^{13}C$ of the modern C_3 plants and provide robust estimates for the isotopic composition of the plant-respired CO_2 at those times.

2.6.3 $\delta^{13}C$ of the Atmospheric CO_2

The $\delta^{13}C$ of atmospheric CO_2 is an important parameter in Cerling's model, but it is also one of the least sensitive (Cerling, Wright, and Vanstone 1992). In earlier studies (Cerling 1991; Andrews, Tandon, and Dennis 1995; Ghosh, Bhattacharya, and Jani 1995), the $\delta^{13}C$ was assumed to be constant and its value was thought to be −6.5‰, equal to the preindustrial atmospheric CO_2 value. However, since then several studies (Mora, Driese, and Colarusso 1996; Thackeray et al. 1990) have demonstrated variation in the $\delta^{13}C$ of atmospheric CO_2 in the past. There are two ways of estimating this $\delta^{13}C$: one based on $\delta^{13}C$ of marine brachiopods (Mora, Driese, and Colarusso 1996), the other based on $\delta^{13}C$ of organic matter (Farquhar, Ehleringer, and Hubick 1989; Thackeray et al. 1990). Since the brachiopod data (Veizer, Fritz, and Jones 1986) show a large scatter, we adopt the second alternative here. Mora, Driese, and Colarusso (1996) observed that the fractionation between atmospheric CO_2 and soil organic matter remained relatively constant between approx 21‰ to 22.5‰ through middle to late Palaeozoic. Ghosh, Ghosh, and Bhattacharya (2001) used this information for estimating the $\delta^{13}C$ of the atmospheric CO_2 from the mean $\delta^{13}C$ of the C_3 organic matter assuming approximately 21‰ fractionation. We note that some workers (Ekart et al. 1999) have assumed a fractionation of 18‰ between $\delta^{13}C$ of atmospheric carbon dioxide and soil organic carbon. However, the magnitude of this fractionation varies significantly with pCO_2 concentration in the atmosphere, which determines the stomatal pore size. Carbon isotope studies of modern plants indicate that increased $[CO_2]$ lowers the plant $\delta^{13}C$ (Gröcke 1998). van de Water, Levitt, and Betancourt (1994) showed that a 30% increase in $[CO_2]$ results in a plant $\delta^{13}C$ shift of −1.5‰. Therefore, in a regime of $[CO_2]$ (Phanerozoic) the atmosphere-plant fractionation is expected to be more than 19‰ (corresponding to modern-day values when average atmospheric $\delta^{13}C$ is −7‰ and average C_3 plant $\delta^{13}C$ is −26‰) as observed in recent atmosphere. The assumed $\delta^{13}C$ shift of 21‰ for our $[CO_2]$ estimation is consistent with this argument. The mean $\delta^{13}C$ of the organic matter from the Motur, Denwa, Tiki, Bagra, and Lameta formations are −23.5‰, −24.6‰, −24.7‰, −26.1‰, and −27.6‰, respectively (see Table 1.1). Therefore, the $\delta^{13}C$ values of the atmospheric CO_2 in those periods are estimated to be −2.5‰, −3.6‰, −3.7‰, −5.1‰, and −6.6‰, respectively. It is interesting to note that there is a systematic decrease in the $\delta^{13}C$ of atmospheric CO_2 from 260 to 65 million years.

2.6.4 Difference Between the Soil [CO_2] and the Atmospheric [CO_2]: S_Z Parameter

The difference in concentration between the soil CO_2 and the atmospheric CO_2 depends on soil temperature, pressure, porosity, and tortuosity; soil respiration rate; and depth of CO_2 production. This difference (S_z) plays an important role in Cerling's mixing model and needs to be assessed independently because of its strong influence on pCO_2 estimate. An approximate value of the soil porosity can be obtained from observations made on recent soils of the same type. However, the mean CO_2 production depth and the soil respiration rate for geologically old soils cannot be estimated with certainty. The rooting depth, the dimensions of the rhizoliths and their density of occurrence in the paleosol profiles may probably be used for such estimation, but no such model is available at present. Observations made on the modern soils show that for the desert soils S_z is less than 3000 ppmV and for well-drained temperate and tropical soils S_z ranges between 5000 and 10,000 ppmV. Mora, Driese, and Colarusso (1996) assumed a value between 3000 and 7000 ppmV for the middle to late Paleozoic semi-arid tropical to temperate vertic paleosols. Some of these paleosols (of the Silurian Age) indicate a very shallow rooting depth. In contrast, Ghosh, Bhattacharya, and Jani (1995) adopted a range between 3000 and 5000 ppmV for the well-drained, semi-arid late Cretaceous paleosols with higher rooting depths than the Silurian soils (Ghosh, Bhattacharya, and Jani 1995; Tandon et al. 1995, 1998; Ghosh, Rudra, and Maulik 1998). We note that the gleyed pedohorizons (signature of clay rich component with less permeability) are, in general, absent in the profiles of the Denwa, Tiki, Bagra, and Lameta formations. Some amount of gleying is present close to the Bk pedohorizons of the Motur and the Denwa formations that may suggest a higher value of S_z. However, the high latitudinal position (60°S) of the study area along with a low mean annual temperature during the Motur time implies reduced plant productivity and consequently low S_z. All the paleosols analyzed in this work show characteristics of well-drained, semi-arid soils. In view of the above considerations, a range of S_z values between 3000 and 5000 ppmV is adopted for these paleosols. However, given the sensitivity of the model to this variable, a critical assessment of its estimation is required.

2.6.5 Calculation of pCO_2 in the Ancient Atmosphere

Using the mean $\delta^{13}C$ values of the paleosol carbonates along with the above-mentioned values of the required parameters and estimated $\delta^{13}C$ of the atmospheric CO_2 based on soil organic matter in the model of Cerling (1991), we have calculated [CO_2] values for the five time windows mentioned above (Ghosh, Ghosh, and Bhattacharya 2001). The values are (in ppmV): 540 to 890 for Motur, 910 to 1510 for Denwa, 880 to 1460 for Tiki, 1675 to 2775 for Bagra, and 1110 to 1850 for Lameta (Table 2.2). The uncertainties in average $\delta^{13}C(OM)$ (see Table 2.1) is not included in the quoted uncertainty of the $[CO_2]$. However, variations in $\delta^{13}C(OM)$ (0.5‰ for Motur and Denwa and 1.2‰ for Tiki and Bagra formations) would change the calculated mean $[CO_2]$ by 20% for Motur and Denwa and 40% for Tiki and Bagra formations, respectively. It is to be noted that the soil samples studied here belong to the same geochemical milieu because they all formed either in the same basin or in a neighboring basin (Tiki) at different times. This implies that the relative CO_2 variation deduced here is expected to be well constrained.

These values represent the first independent estimates of atmospheric CO_2 level during 260 to 65 million years based on soils formed in a Gondwana continent located in the Southern Hemisphere. This is considered an important period in the evolution model (GEOCARB III) since it predicts an increase in the CO_2 level after the low in the early Permian (310–285 millin years ago) and ascribes it to the enhanced rate of degassing. This prediction is verified by our results, but the detailed nature of variation is found to be slightly different. Fig. 2.9 shows a plot of CO_2 concentration in ppm against age, in million years ago. It is seen that there is excellent agreement of derived concentrations with

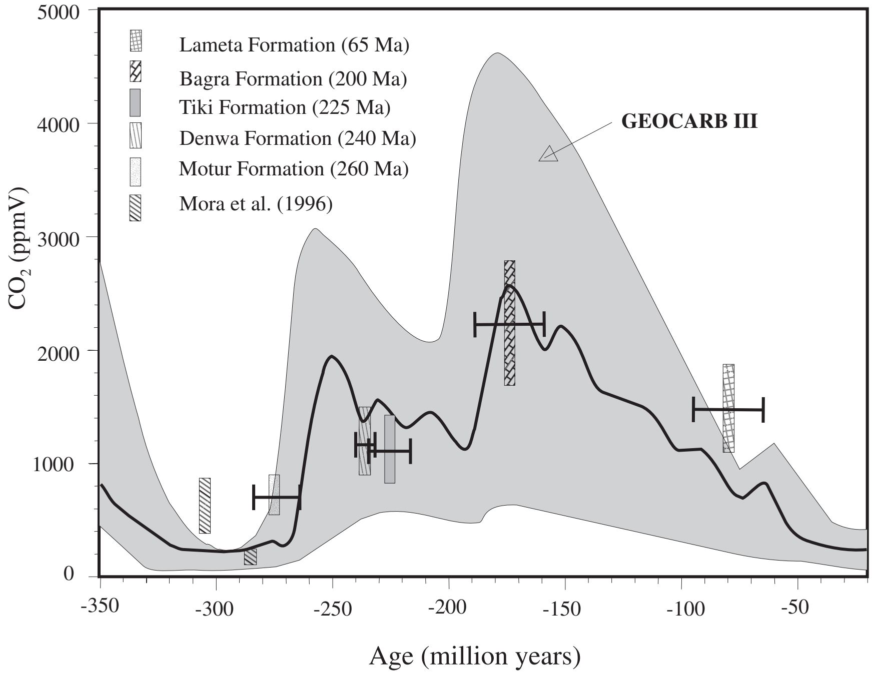

Figure 2.9. Estimated concentration of atmospheric CO_2 (expressed relative to present-day concentration) as a function of time. The points are based on isotopic analysis of pedogenic carbonates. The dashed curve along with envelope (error range) is obtained from GEOCARB III (Berner and Kothavala 2001).

the prediction of Berner and Kothavala (2001) prediction, which was between 275 and 160 million years ago (corresponding to ages of Motur, Denwa, Tiki, and Bagra formations). The abundance of carbon dioxide for 80 million years (Lameta), however, is 1480 ppm in contrast to the prediction of Berner and Kothaval (2001) estimate of about 1000 ppm. The disagreement persists even at the lower limit of our estimate. In this context, it is to be noted that all available evidence indicates very high CO_2 concentrations in the middle Cretaceous to late Cretaceous atmosphere. Emiliani (1995) points out that middle Cretaceous was characterized by widespread anoxia, huge marine ingression indicating active mid-ocean ridges, and warm oceans. All these factors indicate a large increase in the CO_2 flux to the atmosphere and consequent exacerbation of the greenhouse effect and vigorous expansion of biotic productivity. Based on these considerations, an upward revision of model CO_2 input flux at late Cretaceous can, therefore, be considered, and this revision lessens the disagreement.

2.7 Summary

The fluvial deposits of Motur (middle Permian), Denwa (late Triassic), Tiki (early Triassic), Bagra (middle Jurassic), and Lameta (late Cretaceous) formations of the Gondwana supergroup in central India contain a number of calcic paleosols. All of these paleosols are characterized by pedogenic carbonates occurring as rhizocretions and glebules. Soil carbonates from several horizons of these formations were analyzed for oxygen and carbon isotopic ratios. Oxygen isotopic ratio is used to infer about the environment of precipitation and paleotemperature. The carbon isotopic composition of these carbonates and the coexisting soil organic matters provided indirect means to determine the isotopic composition and the partial pressure of atmospheric CO_2 using the CO_2 paleobarometer model of Cerling (1991). The estimate shows that the concentration of CO_2 was low ($\sim$710 ppmV) during the early Permian (275 ± 15 million years ago) followed by continuous rise during the middle Triassic ($\sim$1215 ppmV at 235 ± 5 million years ago), late Triassic ($\sim$1170 ppmV at 225 ± 15 million years ago), and the Jurassic ($\sim$2240 ppmV at 175 ± 30 million years ago) (see Table 2.2 and Fig. 2.9). It is seen that the CO_2 level increased by a factor of 8 from the Permian to the Jurassic and declined again during the Cretaceous. The nature of the change agrees well with the result of the CO_2 evolution model of Berner (GEOCARB III) except that the magnitude of the CO_2 increase in the late Cretaceous was slightly higher than the predicted value. The late Cretaceous [CO_2] estimate is approx 1480 ppmV, higher than the predicted concentration (1000 ppmV). Degassing of Earth's interior caused by the rapid breaking up of the Gondwana landmass during the Triassic and Jurassic periods could have caused the rapid evolution of CO_2; subsequent biotic proliferation in the Cretaceous probably lead to its slight decline.

References

Anderson, J.M. 1981. World Permo-Triassic correlations: Their biostratigraphic basis. In *Gondwana Five,* ed. M.M. Cresswell and P. Vella, 3–10. Rotterdam: A.A. Balkema.

Andrews, J.E., S.K. Tandon, and P.F. Dennis. 1995. Concentration of carbon dioxide in the late Cretaceous atmosphere. *Journal of Geological Society London* 152:1–3.

Bandyopadhyay, S., and D.P. Sengupta.1998. Middle Triassic vertebrate from India. *Gondwana 10, Cape Town. Journal of African Earth Sciences* 27:16–17.

Barnola, J.M., D. Raynaud, Y.S. Korotkevitch, and C. Lorius.1987. Vostok ice core: A 160,000 years' record of atmospheric CO_2. *Nature* 329:408–14.

Baver, L.D., W.H. Gardner, and W.R. Gardner. 1972. *Soil physics*. New York: John Wiley.

Berner, R.A. 1991. A model for atmospheric CO_2 over Phanerozoic time. *American Journal of Science* 291:339–76.

———. 1994. GEOCARBII: A revised model of atmospheric CO_2 over Phanerozoic time. *American Journal of Science* 294:56–91.

———. 1997. The rise of plants and their effect on weathering and atmospheric CO_2. *Science* 276:544–45.

Berner, R.A., and Z. Kothavala. 2001. GEOCARB III: A revised model of atmospheric CO_2 over Phanerozoic time. *American Journal of Science* 301:182–204.

Casshyap, S.M., and H.A. Qidwai. 1971. Paleocurrent analysis of Lower Gondwana sedimentary rocks, Pench Valley Coalfield, Madhya Pradesh [India]. *Journal Geological Society of India* 5:135–45.

Casshyap, S.M., and R.C. Tewari. 1988. Depositional model and tectonic evolution of Gondwana basins: Lucknow. *Palaeobotanist* 36:59–66.

Casshyap, S.M., R.C. Tewari, and A. Khan. 1993. Alluvial fan origin of the Bagra Formation (Mesozoic Gondwana) and tectono-stratigraphic implications. *Journal Geological Society of India* 42:269–79.

Cerling, T.E. 1984. The stable isotopic composition of modern soil carbonate and its relationship with climate. *Earth Planetary Science Letters* 71:229–40.

———. 1991. Carbon dioxide in the atmosphere: Evidence from Cenozoic and Mesozoic palaeosols. *American Journal of Science* 291:377–400.

———. 1999. Stable carbon isotopes in palaeosol carbonates. In *Palaeoweathering, palaeosurfaces, and related continental deposits,* ed. M. Thirty and Simm-Coincon, 43–60. Oxford: Blackwells.

Cerling, T.E., and J. Quade. 1993. Stable carbon and oxygen isotopes in soil carbonates. In *Climate change in continental isotopic records,* ed. P.K. Swart, C. Lohmann, C. Kyger, J.A. McKenzie, and S. Savin, 217–31. Washington, D.C.: American Geophysical Union.

Cerling, T.E., J. Quade, Y. Wang, and J.R. Bowman. 1989. Carbon isotopes in soils and palaeosols as ecology and palaeoecology indicators. *Nature* 341:138–39.

Cerling T.E, V.P. Wright, and S.D. Vanstone. 1992. Further comments on using carbon isotopes in paleosols to estimate the CO_2 content of the palaeo-atmosphere. *Journal of the Geological Society of London* 149: 673–76.

Chatterjee, S. and T. Roychowdhury. 1974. Triassic Gondwana vertebrates from India. *Indian Journal of Earth Sciences* 11:96–112.

Crowley, T.J., and R.A. Berner. 2001. CO_2 and climate change. *Science* 292:870–72.

Deines, P., D. Langmuir, and R.S. Harmon. 1974. Stable carbon isotope ratios and existence of a gas phase in the evolution of carbonate ground waters. *Geochimica Cosmochimica Acta* 38:1147–164.

Driese, S.G., and C.I. Mora. 1993. Physico-chemical environment of pedogenic carbonate formation in Devonian vertic palaeosols, central appalachians, USA. *Sedimentology* 40:199–216.

Dutta, P.M., and D.P. Das. 1996. Discovery of the oldest fossil mammal from India. *Indian Minerals* 50:217–22.

Ehleringer, J.R. 1989. Carbon isotope ratios and physiological processes in arid land plants. In *Stable isotopes in ecological research,* ed. P.W. Rundel, J.R. Ehleringer, and K.A. Nagy. New York: Springer-Verlag.

Ekart, D.D., T.E. Cerling, I.P. Montanez, and N.J. Tabor. 1999. A 400 million year carbon isotope record of pedogenic carbonate: Implications for paleoatmospheric carbon dioxide. *American Journal of Science* 299:805–27.

Emiliani, C. 1995. Planet Earth: *cosmology, geology, and the evolution of life and environment,* ed. C. Emiliani, 718. Cambridge University Press.

Farquhar, G.D., J.R. Ehleringer, and K.T. Hubick. 1989. Carbon isotope discrimination and photosynthesis. *Annual Review of Plant Physiology and Plant Molecular Biology* 40:503–37.

Ghosh, P. 1997. Geomorphology and palaeoclimatology of some Upper Cretaceous palaeosols in central India. *Sedimentary Geology* 110:25–49.

Ghosh, P., S.K. Bhattacharya, and R.A. Jani. 1995. Palaeoclimate and palaeovegetation in central India during the Upper Cretaceous based on stable isotope composition of the palaeosol carbonates. *Palaeogeography, Palaeoclimatology, Palaeoecology* 114: 285–96.

Ghosh, P., P. Ghosh, and S.K. Bhattacharya. 2001. CO_2 levels in the late Paleozoic and Mesozoic atmosphere from soil carbonate and organic matter, Satpura basin, Central India. *Palaeogeography, Palaeoclimatology, Palaeoecology* 170:219–36.

Ghosh P., D.K. Rudra, and P. Maulik. 1998. Palaeoclimatic indicators in the Satpura Gondwana succession, India, Gondwana 10. *Journal of African Earth Sciences* 27: 1A.

Gröcke, D.R. 1998. Carbon-isotope analyses of fossil plants as a chemostratigraphic and palaeo-environmental tool. *Lethaia* 31:1–13.

Houghton, R.A., and G.M. Wood. 1989. Global climate change. *Scientific American* 260: 36–44.

IAEA/WMO. 1998. *The GNIP [Global network for isotopes in precipitation] database, Release 2*. International Atomic Energy Agency.

IPCC. 1990. *Climate change: The IPCC scientific assessment,* ed. J.T. Houghton, B.A. Callander, and S.K. Varney, 200. Cambridge, U.K.: Cambridge University Press.

Keeling, C.D. 1994. Global historical CO_2 emissions. In *Trends '93: A compendium of data on global change,* ed. T.A. Boden, D.P. Kaiser, R.J. Sepanski, F.W. Stoss, and F.W. Logsdon, 501–505. Springfield, Va.: American Geological Institute.

Kirkham, D., and W.L. Powers. 1972. *Advanced soil physics*. New York: Wiley-Interscience.

Kutty, T.S., S.L. Jain, and T. Roychowdhury. 1998. Gondwana sequence of the northern Pranhita-Godavari Valley: Its stratigraphy and vertebrate faunas. *Palaeobotanist* 36: 214–29.

Kutzbach, J.E., and R.G. Gallimore. 1989. Pangean climates: Megamonsoons of the megacontinent. *Journal of Geophysical Research* 94:3341–357.

McElwain, J.C., and W.G. Chaloner. 1996. The fossil cuticle as a skeletal record of environmental change. *Palaios* 11:376–88.

Mora, C.I., S.G. Driese, and L.A. Colarusso. 1996. Middle to late Paleozoic atmospheric CO_2 levels from soil carbonate and organic matter. *Science* 271:1105–107.

Mora, C.I., D.E. Fastovsky, and S.G. Driese. 1993. Geochemistry and stable isotopes of palaeosols, 66. A Geological Society of America Continuing Education Short Course.

Mora, C.I., B.T. Sheldon, C.W. Elliott, and S.G. Driese. 1998. An oxygen isotope study of illite and calcite in three Appalachian Paleozoic vertic paleosols. *Journal Sedimentary Research* 68:456–64.

Mukherjee, R.N., and D.P. Sengupta. 1998. New capitosaurid amphibians from the middle Triassic Denwa Formation of Satpura Gondwanas, central India. *Alcheringa* 22: 317–27.

Raja Rao, C.S., ed. 1983. Coalfields of India: Coal resouces of Madhya Pradesh, Jammu, and Kashmir. Geological Society of India Bulletin 3:195–98.

Robinson, P.L. 1967. The Indian Gondwana formations: A review. In *Gondwana stratigraphy, International Union of Geological Sciences Symposium, Buenos Aires, 1–15 October 1967,* ed. A.J. Amos, 201–68. Paris: United Nations Educational, Scientific, and Cultural Organizations.

Royer, D.L., R.A. Berner, and D.J. Beerling. 2001. Phanerozoic atmospheric CO_2 change: Evaluating geochemical and paleobiological approaches. *Earth Science Reviews* 54: 349–92.

Rozanski, K., L.A. Araguas, and R. Gonfiantini. 1993. Isotopic patterns in modern global precipitation. In: *Continental isotope indicators of climate,* geophysical monograph 78:1–35. Washington, D.C.: American Geophysical Union.

Sahni, A., S.K. Tandon, A. Jolly, S. Bajpai, A. Sood, and S. Srinivasan. 1994. Cretaceous dinosaur eggs and nesting sites from the Deccan volcano-sedimentary province of peninsular India. In *Dinosaur eggs and babies,* ed. K. Carpenter, K. Hirsch, and J. Horner. New York: Cambridge University Press.

Sarkar, A., S.K. Bhattacharya, and D.M. Mohabey. 1991. Stable isotope analyses of dinosaurs egg shells: Paleoenvironmental implications. *Geology* 19:1068–71.

Sarkar, A., R. Ramesh, and S.K. Bhattacharya. 1990. Effect of sample pretreatment and size fraction on the $\delta^{18}O$ and $\delta^{13}C$ values of foraminifera in Arabian Sea sediments. *Terra Nova* 2:489–93.

Sastry, M.V.A., S.K. Acharya, S.C. Shah, P.P. Satsangi, P.K. Raha, G. Singh, and R.M. Ghosh, eds. 1977. Stratigraphic lexicon of Gondwana formations of India. *Geological Survey of India* (miscellaneous publication) 36:13–15.

Satsangi, P.P. 1988. Vertebrate fauna from the Indian Gondwana Sequence. *Paleobotanist* 36:245–53.

Scotese, C.R. 1997. *Paleogeographic atlas.* PALEOMAP progress report 90-0497, 45. Arlington, Tex.: Department of Geology, University of Texas at Arlington.

———. 1998. Gondwana's climate changes. Abstract in *Journal of African Earth Sciences* 27:172–73.

Sengupta, D.P. 1992. Metoposaurus maleriensis Roychowdhury from the Tiki formation of the Son-Mahanadi valley of central India. *Indian Journal of Geology* 64:300–305.

Singh, G., and R.M. Ghosh. 1977. Bagra conglomerate. In Stratigraphic lexicon of Gondwana formations of India, ed. Sastry et al. *Geological Survey India* (miscellaneous publication) 36:13–15.

Soil Survey Staff. 1975. Soil Taxonomy. *Soil Conservation Survey.* Handbook 436. U.S. Department of Agriculture.

Sundaram, D., A. Maiti, A., and G. Singh. 1979. Upper Triassic microflora from Tiki formation of South Rewa Gondwana basin, Madhya Pradesh, India. In *Fourth international Gondwana symposium: Delhi, India* 1:511–14, ed. B. Laskar and C.S. Raja. Delhi, India: Hindustan Publishing Corp.

Tajika, E., and T. Matsui. 1992. Evolution of terrestrial proto-CO_2 atmosphere coupled with thermal history of the earth. *Earth and Planetary Science Letters* 113:251–66.

Tandon, S.K., and J.E. Andrews. 2001. Lithofacies associations and stable isotopes of palustrine and calcrete carbonates: Examples from an Indian Maastrichtian regolith. *Sedimentology* 48(2):339–55.

Tandon, S.K., J.E. Andrews, A. Sood, and S. Mittal. 1998. Shrinkage and sediment supply control on multiple calcrete profile development: A case study from the Maastrichtian of central India. *Sedimentary Geology* 119:25–45.

Tandon, S.K., A. Sood, J.E. Andrews, and P.F. Dennis. 1995. Palaeoenvironments of the dinosaur-bearing lameta beds (Maastrichtian), Narmada valley, central India. *Palaeogeography, Palaeoclimatology, Palaeoecology* 117:123–54.

Thackeray, J.F., N.J. van der Merwe, J.A. Thorp-Lee, A. Sillen, J.L. Lanham, R. Smith,

A. Keyser, and P.M.S. Monteiro. 1990. Changes in carbon isotope ratios in the late Permian recorded in the therapsid tooth apatite. *Nature* 347:751–53.

van de Water, P.K., S.W. Leavitt, and J.L. Betancourt. 1994. Trends in stomatal density and $^{13}C/^{12}C$ ratios of *Pinus flexilis* needles during last glacial-interglacial cycles. *Science* 264:239–43.

Veevers, J.J, and R.C. Tewari. 1995. Gondwana master basin of peninsular India between Tethys and the interior of the Gondwanaland province of Pangea. *Geological Society of America* (memoir) 187:1–72.

Veizer, J., P. Fritz, and B. Jones. 1986. Geochemistry of brachiopods: Oxygen and carbon isotopic records of Paleozoic oceans. *Geochimica et Cosmochimica Acta* 50:1679–96.

Yapp, C.J., and H. Poths. 1992. Ancient atmospheric CO_2 pressures inferred from natural goethites. *Nature* 355:342–44.